ECCOMAS Computational Fluid Dynamics Conference 2001
Swansea, Wales, UK, 4-7 September 2001

THREE-DIMENSIONAL FLUID-STRUCTURE INTERACTION MODELLING OF BLOOD FLOW IN ELASTIC ARTERIES

Esko Järvinen, Mikko Lyly, Juha Ruokolainen, Peter Råback

CSC - Scientific Computing Ltd.
P. O. Box 405, FIN - 02101, Espoo, Finland
web page: http://www.csc.fi

Key words: Hemodynamics, artery, fluid-structure interaction, finite element method, computer modelling

Abstract. *This paper presents a scheme for the loosely coupled modelling of fluid-structure interaction in the elastic artery. The scheme is tested with a simple 3D test case of propagating pressure pulse in an artery. Qualitative agreement with the physiologically correct features of the pulsatile flow in an elastic artery were obtained. The computations were carried out by using an in-house finite element based solver. The blood was modelled as an incompressible, Newtonian fluid. The artery model was based on nonlinear elasticity, and the coupling of the fluid and the solid were based on an algorithm using ALE formulation. The systems of nonlinear equations were solved using a parallel supercomputer.*

1 INTRODUCTION

Cardiovascular diseases remain the leading cause of death in the industrialized countries [1]. Considerable evidence exists that fluid mechanical forces have a strong influence on the initiation and progression of several cardiovascular diseases, *e.g.,* atherosclerotic and ischemic diseases [2, 3]. Early events in the atherosclerotic process are strongly characterized by the interaction of the flow and the vessel [4, 5, 6]. The vessel wall mechanics is considered to have also a strong influence on these processes [7, 8].

The large arteries of the human body behave as cushions, softening the pulsatile flow generated by the contracting left ventricle of the heart into a steady flow in the periferial arteries. The arterial walls are viscoelastic in nature. Stiffened artery walls can disorder this rhythmic interaction between the heart and the artery, increasing the speed of the pressure pulses propagating in the circulatory system. In a stiffened aorta, the pressure pulse reflects from the periferial circulation sooner, causing abnormal systolic blood pressure and higher left ventricular afterload [9].

The flowing substance, blood, also has some special characteristics. Blood is a non-Newtonian multiphase substance, which is slightly shear-thinning and viscoelastic [10]. Blood is a suspension of red cells, white cells, platelets and the plasma. The viscosity of blood depends on the proportion of the particulate matter, which normally account for about 40-45 per cent by volume of the blood. Nevertheless, it is well known that in large arteries at moderate or high shear rates blood behaves as a Newtonian fluid [10].

Computational modelling offers a powerful tool to analyze basic relations between various solid and fluid mechanical parameters in the circulatory system. Computational approaches ranging from simple lumped models to full 3D simulations have been used. The advantage of the lumped models is the capability to simulate an entire human cardiovascular system as a set of ordinary differential equations, often represented by analogy to electrical circuits [12, 13]. In quasi-1D model the distensibility of the vessels can also be taken into acount [14]. Along with the increased availability of powerful computer facilities, three dimensional modelling has become more popular. The advantage of these models is their capability to produce detailed knowledge about the time-dependent flow characteristics of the system. However, these models are computationally far too intensive to be used in the analysis of a larger part of the circulatory system. Such models have therefore usually been limited to tackle smaller subjects, like a single carotid or coronary artery bifurcation.

The computation of unsteady flows in the circulatory system become even more time-consuming when the distensibility of the vessels is taken into account. Earlier computations have often been done using mostly rigid geometries. During the last decade, an increasing number of articles concidering the fluid-structure interactive (FSI) models of pulsatile blood flow in the elastic vessel have been published, see *e.g.* [15, 16, 17, 18, 19].

In some of these papers, the effect of wall distensibility is observed to have only a minor influence, for example, on the overall structure of the flow patterns. However, we believe that in many cases the elasticity can not be neglected in the study of pulsatile flow in the cardiovascular system. The elasticity most obviously has an important role in the analysis of the endothelial cell dysfunction mechanism, pressure pulse propagation in a conduit, interaction of the heart and the systemic circulation, pulsatile flow passing an anastomosis or a severe stenotic artery, mechanical interaction of stent and the vessel wall, or interaction between tissues with different material characteristics.

The purpose of the present study was to construct a loosely coupled computational fluid-structure interaction scheme for modelling pulsatile flow in an elastic artery. In this paper, we start by representing the mathematical foundation for the FSI problem. The computations were carried out by using an in-house finite element based solver called ELMER. The blood was modelled as an incompressible and Newtonian fluid. The artery model was based on nonlinear elasticity and the coupling of the fluid and the solid models was based on an algorithm using ALE formulation. The systems of nonlinear equations were solved using parallel supercomputer. Finally, the results with a simple test case are presented and discussed.

2 COUPLED FLUID-STRUCTURE PROBLEM

Let $\Omega_F(0) \subset \mathbb{R}^3$ and $\Omega_S(0) \subset \mathbb{R}^3$ be open bounded domains representing the undeformed configurations of the fluid and solid at rest, respectively. The interface boundary which initially separates the domains is denoted by $\Gamma_{FS}(0) = \partial\Omega_F(0) \cap \partial\Omega_S(0)$, see Figure 1 below.

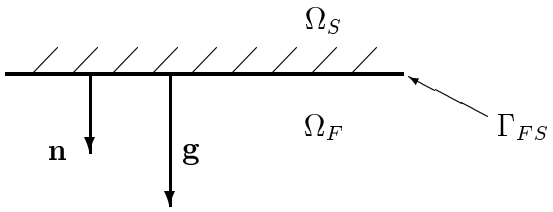

Figure 1: Interface surface between wall and fluid.

Deformation of the solid. The mathematical model which describes the mechanical behaviour of the solid consists of the equilibrium equations

$$\rho \frac{\partial^2 u}{\partial t^2} - \nabla \cdot \tau = f \quad \text{in } \Omega_S(0) \tag{1}$$

and

$$n \cdot \tau = g \quad \text{on } \Gamma_{FS}(0), \tag{2}$$

where $u(x,t)$ is the unknown displacement vector, $\rho(x)$ is the density of the material, $f(x,t)$ is the body force and $g(x,t)$ the boundary traction. The vector $n(x)$ is the unit outward normal to the boundary. The stress tensor $\tau(x,t)$ depends on the displacement through the following definitions (see *e.g.* [20] for more details):

$$\begin{cases} \varphi := x + u & \text{Deformation (motion)} \\ F := \nabla\varphi & \text{Deformation gradient} \\ E := \frac{1}{2}(F^T F - I) & \text{Green-StVenant strain} \\ \sigma := C : E & 2^{nd} \text{ Piola-Kirchhoff stress} \\ \tau := F \cdot \sigma & 1^{st} \text{ Piola-Kirchhoff stress} \end{cases}$$

The deformed configurations of the solid and interface boundary are defined for $t > 0$ as

$$\Omega_S(t) = \{y \in \mathbb{R}^3 \mid y = \varphi(x,t),\ x \in \Omega_S(0)\}$$

and

$$\Gamma_{FS}(t) = \{y \in \mathbb{R}^3 \mid y = \varphi(x,t),\ x \in \Gamma_{FS}(0)\}.$$

For homogenic and isotropic materials the fourth order elasticity tensor C is defined in terms of the Lamé parameters λ and μ as

$$C : E = 2\mu E + \lambda \mathrm{tr}(E) I. \tag{3}$$

Deformation of the fluid domain. Next, since our FSI-model will be based on an ALE-formulation, we have to construct a one-to-one map which associates the reference configuration $\Omega_F(0)$ to the actual domain $\Omega_F(t)$ for $t > 0$. As the evolution of the fluid domain is completely characterized by the movement of the interface boundary, it suffices to extend the displacement of the solid in an appropriate way from $\Gamma_{FS}(0)$ to $\Omega_F(0)$, define the deformation map as $\varphi = x + u$ in $\Omega_F(0)$, and to write

$$\Omega_F(t) = \{y \in \mathbb{R}^3 \mid y = \varphi(x,t),\ x \in \Omega_F(0)\}.$$

The extension of the displacement can be defined freely as long as the corresponding deformation is continuous, orientation preserving, and sufficiently smooth. One possibility here is to use the harmonic extension, *i.e.*, $\Delta u = 0$ with the Laplace operator applied componentwise. A more practical extension is obtained from the linear elasticity equation

$$\nabla \cdot C : \varepsilon(u) = 0 \quad \text{in } \Omega_F(0), \tag{4}$$

where C is the elasticity tensor and $\varepsilon(u) = \frac{1}{2}(\nabla u^T + \nabla u)$ the linearized strain tensor. The numerical examples will be given using Equation (4) with C defined by Equation (3).

Fluid flow. The fluid flow is characterized by the unsteady incompressible Navier-Stokes equations which we write in an Arbitrary-Lagrangian-Eulerian (ALE) formulation as follows (*cf.* [21] for more details):

$$\rho \left(\frac{\partial v}{\partial t} + (v \cdot \nabla)v - (V \cdot \nabla)v \right) - \nabla \cdot \sigma = f \quad \text{in } \Omega_F(t) \tag{5}$$

and

$$\nabla \cdot v = 0 \quad \text{in } \Omega_F(t), \tag{6}$$

where $v(x,t)$ is the unknown fluid velocity vector, $V(x,t) := \frac{\partial}{\partial t} u(\varphi^{-1}(x,t),t)$ is the known deformation velocity (also referred to as the "mesh velocity"), $f(x,t)$ is the body force and $\sigma(x,t)$ the stress tensor. For Newtonian fluids the stress is defined as

$$\sigma = 2\mu\, \varepsilon(v) - pI,$$

where $p(x,t)$ is the pressure, μ the viscosity, and $\varepsilon(v)$ the linear strain rate tensor.

We assume that no slipping occures between the wall and the fluid, *i.e.*,

$$v = V \quad \text{on } \Gamma_{FS}(t).$$

From the solution σ we finally compute the boundary traction g in Equation (2) as

$$g(x,t) = n \cdot \sigma(\varphi(x,t),t) \quad \text{on } \Gamma_{FS}(0). \tag{7}$$

Pulse wave propagation and arterial compliance. The distensibility of the arterial wall has a major influence on the nature of the waveform within elastic conduit. In addition to the discontinuities in the anatomy (*e.g.*, bifurcations or stenoses), the compliance of the vessel governs the pulse wave propagation in the circulatory system. Since in this work we consider pulsatile flow in an elastic tube, for the validation of the computed results we need to choose some measurable quantities which characterize the dynamics deforming system. The pulse wave velocity in an elastic tube can be estimated by the Moens-Korteweg equation [11]

$$c_0 = \sqrt{\frac{E\,h}{2\,R\,\rho_f}} \tag{8}$$

where c_0 is the pulse wave velocity, E is the Young's modulus of the vessel, h is the tube wall thickness, ρ_f is the fluid density and R is the radius of the tube. The compliance of an elastic artery, C, can be presented as the slope of the area-pressure relation

$$C = \frac{\Delta A}{\Delta p} \tag{9}$$

where ΔA and Δp are the differences between the tube maximal and minimal lumen areas and the pressure during the pulse cycle, respectively.

Numerical methods and the coupling algorithm. The equations of the fluid flow and the solid wall are solved iteratively with the sequential algorithm illustrated in Figure 2.

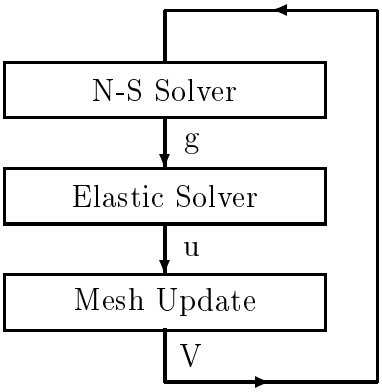

Figure 2: Sequential algorithm

To be more spesific, the iteration procedure consists of time integration and three nested iteration loops (weak coupling):

- Discretize the problem implicitely in time using Newmark's method and backward differences. For each time step:
- Split the system into a sequence of uncoupled subproblems by Gauss-Seidel-type iteration depicted in Figure 2. For each iteration:
- Solve the nonlinear subproblems iteratively by successive linearizations using Picard and Newton iterations. For each linearization:
- Discretize the linearized equations by domain decomposition and adaptive stabilized finite element methods [22]. Solve the algebraic systems iteratively in parallel by appropriate Krylov space methods (CG and BiCGStab).

The outer relaxation loop is terminated when the accuracy of the solution reaches the steady state convergence tolerance, T_{SS}, defined by the user. The middle loop is terminated when the error gets smaller than the nonlinear system convergence tolerance, T_{NL}. The stopping criterion for the inner iteration is given by the linear system convergence tolerance, T_L. By choosing these parameters properly with respect to the mesh parameters and time step sizes, the accuracy of the numerical solution can be flexibly controlled. For the iteration illustrated in Figure 2, relaxation was applied to the traction force g and to the displacement u.

Parallel implementation. A domain decomposition method has been used to solve all the equations in parallel processing. The first step of the parallel algorithm is the partitioning of the finite element mesh discretizing the computational domain, see Figure 3. The domain is partitioned to subdomains of approximately equal size to achieve proper load balancing. The linearized equations are assembled and solved using these partitioned meshes.

Each node of the partitioned mesh is assigned to a processor which owns the nodal point. The nodal points are either interface nodes or inside a partition. The parts of the linear equation coefficient matrices and right hand side vectors which are internal to a partition are assembled as usual. The interface parts of the matrices are assembled separately and distributed among processors sharing the nodal points on the interfaces. After the assembly, the solution to the linear equations is obtained using an iterative solver. In the current work, the solution algorithm was a BiCGStab based iterative solver using block ILU as the preconditioner.

The parallel implementation of this algorithm is quite simple, and requires only the following parts of the algorithm to be parallelized:

- Sending and receiving the interface parts of the matrices and vectors
- Matrix-vector multiplication
- Vector norm
- Vector dot product

The implementation uses the MPI (Message Passing Interface), which makes it portable across wide range of hardware platforms.

3 A NUMERICAL EXAMPLE

To validate the numerical model described in Section 2, a simple test case of propagating pressure pulse in a straight tube was used. The diameter, wall thickness and the material characteristics of the tube were chosen to correspond to a human thoraic aorta reported by Lang *et al.* [23]. They had measured instantaneous aortic cross-section area of proximal descending thoraic aorta of several patients with echocardiography.

Model dimensions and size. The length of the tube was 0.1 m, inner radius 10.2 mm and the thickness of the wall 1.8 mm. To reduce computational time, only a 90-degree cross section of the tube was used and symmetry assumed. The finite element mesh is shown in Figure 3. The mesh consisted of 1760 and 4434 linear elements for the solid and the fluid, respectively. The total number of nodes was 5637.

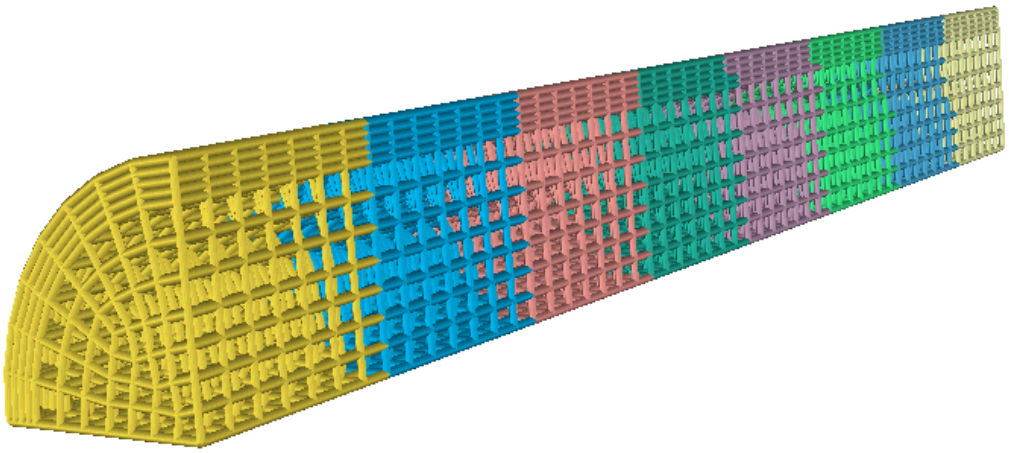

Figure 3: Computational mesh and mesh division for parallel processing.

Material characteristics. The wall density was 1150 kg/m^3, Young's modulus for the vessel wall $3.0 \cdot 10^5$ Pa, blood density 1050 kg/m^3 and blood viscosity $4.0 \cdot 10^{-3}$ Pa s. Poisson ratio for the elastic artery was 0.3.

Boundary conditions. On the vertical and horizontal symmetry planes of the quarter section of the tube, the displacements of the mesh and the velocities of the fluid were set to zero in the normal directions of the planes. At the inlet and outlet of the tube, the fluid velocities tangential to the planes, as well as the displacements of the mesh in the axial direction, were set to zero. A pressure pulse shown in Figure 4 was applied at the inlet of the tube.

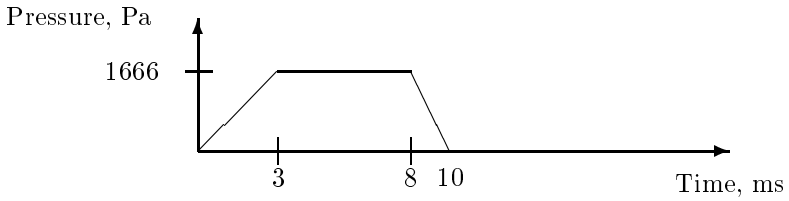

Figure 4: Pressure pulse at the inlet.

Time-stepping and convergence tolerances. The total simulation time was 25 ms and the timestep was 1 ms. Convergence tolerances were $T_{SS} = 10^{-4}$, $T_{NL} = 10^{-4}$, $T_L = 10^{-6}$ and relaxation factor was 0.1 for both the fluid and the solid solvers.

The computation was done with 8 processors on SGI Origin 2000 machine. The mesh division is illustrated in Figure 3. The total cpu-time per timestep was 3.2 hours, corresponding 0.4 hours per processor. The total cpu-time was 80.0 hours and the processing time 10.3 hours. Due to the long computing time, the comparison to a single processor run was done by a simulation with only 5 timesteps. For the single processor run, the cpu-time per timestep was 1.2 hours. Hence, the speedup of 3.0 was achived.

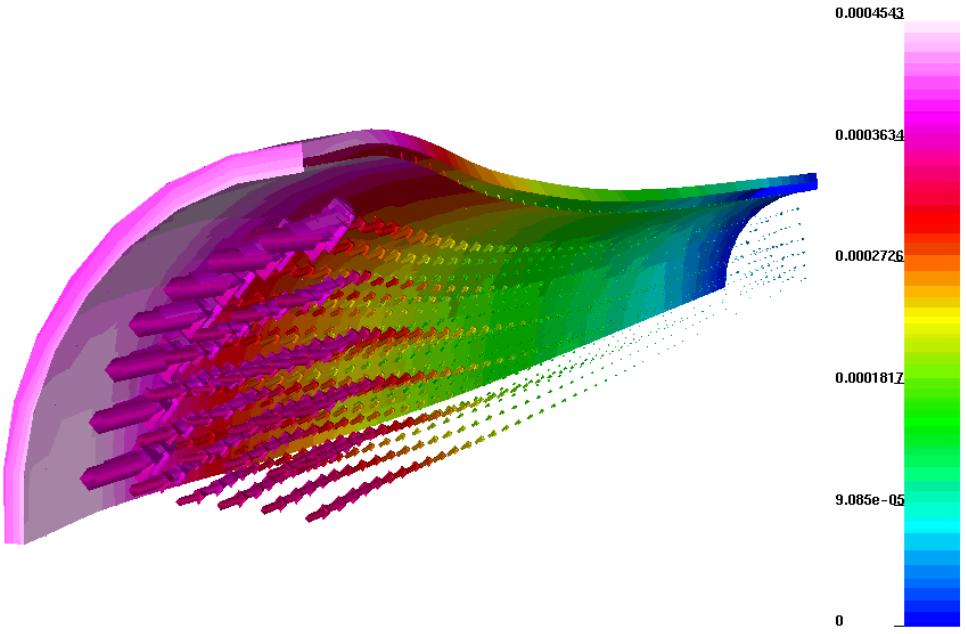

Figure 5: Wall displacement at t = 7 ms. The displacement of the structure has been magnified by a factor of 20. The unit of the scale is meter.

In Figure 5 the enlargement of the tube at the inlet is shown at the phase of the maximum pressure $p = 1666\ Pa$. The maximum displacement at the wall was 0.4543 mm, which corresponds to compliance C = 0.24 cm^2/mmHg, defined by Equation 9.

In the figure 6 the velocity fields and pressure isosurfaces at different timestages are shown. After the injection of the pressure pulse (t > 10 ms) the pulse is propagating through the tube, roughly estimated by the velocity of 6 m/s. At the outlet there is an

unrealistic backward reflection of the pulse caused by the unproper numerical approximation of the boundary condition. There exists some outflow at the inlet during the simulation.

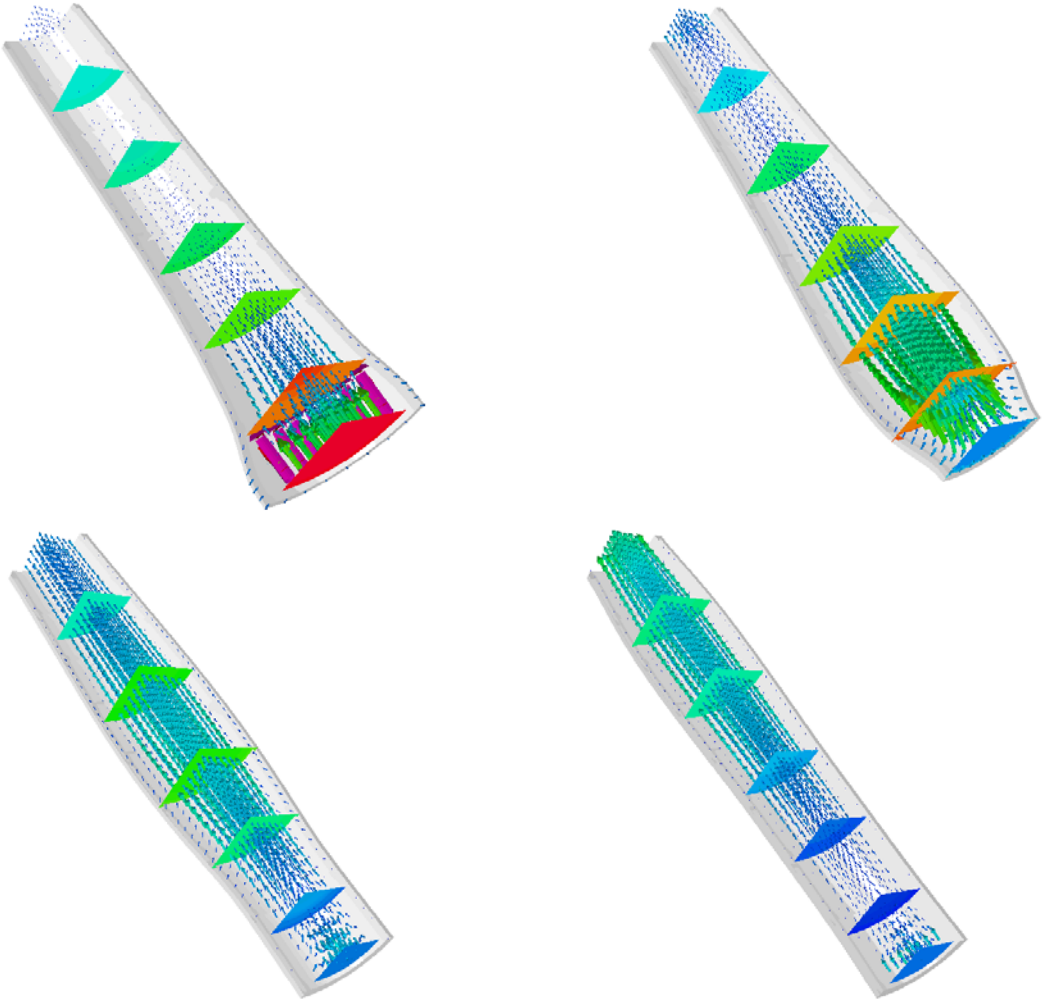

Figure 6: Velocity fields and pressure isosurfaces on timesteps t = 5, 10, 15 and 20 ms. The displacements of the structure have been magnified by a factor of 20.

4 DISCUSSIONS

The results with a test case presented in Section 3 show that the current model gives a qualitatively realistic results for the pulse injection and propagation in an elastic tube. Both the pressure and the velocity pulses are propagating through the tube with a finite velocity. The Moens-Korteweg equation (Eq. 8) gives an estimate of 5.0 m/s (in the sim-

ulation 6 m/s) for the speed of the propagating pulse. In the Lang *et al. in vivo* measurements, the compliance (Eq. 9) was 0.23 cm^2/mmHg (in the simulation 0.24 cm^2/mmHg).

However, at this stage of the work with the current model, a detailed comparison of the computed results with the measurements is not yet relevant for several reasons. In our computations, the inlet boundary condition is not realistic. In a real physilogical system, the maximum pressure at the end of the systolic phase of the contracting heart, is higher (the difference between systolic and the diastolic pressure is about $\Delta \mathrm{p} = 30...40\mathrm{mmHg}$) and it is reached slower, approximately in 100ms, than in the simulation. In the physiological system, due to the inertia of the fluid, there exists also a phase shift between the pressure and the velocity pulses [11].

There are several other fundamental shortcomings to be overcome in the current analysis, regarding the modelling of a physiologically realistic system. The wall model should be modified to correspond better with the nonlinear viscoelastic character of the arterial wall, a feature clearly seen also in Lang *et al.* measurements. The outlet boundary condition should be improved to function without any unrealistic numerical reflections and, further on, it should be capable to link the current model with the separate lower level model (1D or lumped) which enables physiologically correct description of the response of the rest of the systemic circulation, see Formaggia *et al.* [19, 24].

Further challages include as well, improvement of the sequential iteration algorithm, illustrated in Figure 2. With such an algorithm, the larger the vessel is, the smaller relaxation factors are needed to achive a convergence, see Nobile [25]. One way to overcome this problem has been proposed by Riemslagh *et al.* [26]. Their solution procedure was based on artificial compressibility.

Even tought the speedup in parallel processing reached in this work was reasonable, the parallel efficiency of our scheme needs to be improved. Finally, the non-Newtonian property of blood should be also taken into account in the modelling of realistic systems, see Gijsen *et al.* [27].

5 CONCLUSIONS

The modelling of the human cardiovascular system is well motivated but a complicated and computationally intensive task. In this work, a basic scheme for the loosely coupled modelling of fluid-structure interaction in the elastic artery was developed and tested with a simple test case. Qualitative agreement with the physiologically realistic features of the pulsatile flow in an elastic artery were obtained.

6 ACKNOWLEDGEMENTS

This work was part of the Academy of Finland, Mathematical Methods and Modelling in the Sciences 2000-2003 research programme.

REFERENCES

[1] World Health Organization (WHO), *http://www.who.int/ncd/cvd/index.htm*

[2] S. A. Berger, L.-D. Jou, *Flow in Stenotic Vessels*, Ann. Rev. Fluid Mech., **32** (347-382), 2000.

[3] D. N. Ku, *Blood Flow in Arteries*, Ann. Rev. of Fluid Mech., **29** (399-434), 1997.

[4] R. M. Nerem, *Vascular Fluid Dynamics, the Arterial Wall, and Atherosclerosis*, J. Biomech. Eng., **114** (274-282), 1992.

[5] O. Traub, B. C. Berk, *Laminar Shear Stress: Mechanisms by which Endothelial Cells Transduce an Atheroprotective Force*, Arteriosclerosis, Thrombosis and Vascular Biology, **18** (677-685), 1998.

[6] P. F. Davies, *Spatial Hemodynamics, the Endothelium, and Focal Atherogenesis: A Cell Cycle Link?*, Circulation Research, **86** (114-), 2000.

[7] A. Delfino, N. Stergiopulos, J. E. Moore, J.-J. Meister, *Residual Strain Effects on the Stress Field in a Thick Wall Finite Element Model of the Human Carotid Bifurcation*, J. Biomech., **30** (777-786), 1997.

[8] Z. Ding, M. H. Friedman, *Dynamics of Human Coronary Arterial Motion and Its Potential Role in Coronary Atherogenesis*, J. Biomech. Eng., **22** (488-492), 2000.

[9] G. M. London, A. P. Guerin, *Influence of Arterial Pulse and Reflected Waves on Blood Pressure and Cardiac Function*, Am. Heart J., **138** (S220-S224), 1999.

[10] Y. C. Fung, *Biomechanics: Mechanical Properties of Living Tissues*, Springer, 1993.

[11] W. W. Nichols, M. F. O'Rourke, *McDonald's Blood Flow in Arteries*, Arnold, 1999.

[12] C. Sheng, S. N. Sarwal, K. C. Watts, A. E. Marble *Computational Simulation of Blood Flow in Human Systemic Circulation Incorporating an External Force Field*, Med. & Biol. Eng. & Comp., **33** (8-17), 1995.

[13] M. Zacek, E. Krause, *Numerical Simulation of the Blood Flow in the Human Cardiovascular System*, J. Biomech., **29** (13-20), 1996.

[14] N. Stergiopulos, D. F. Young, T. R. Rogge, *Computer Simulation of Arterial Flow with Applications to Arterial and Aortic Stenoses*, J. of Biomech., **25** (1477-1488), 1992.

[15] K. Perktold, G. Rappitsch, *Computer Simulation of Local Blood Flow and Vessel Mechanics in a Compliant Carotid Artery Bifurcation Model*, J. Biomech., **28** (845-856), 1995.

[16] S. Z. Zhao, X. Y. Xy, M. W. Collins, *The Numerical Analysis of Fluid-Solid Interactions for Blood Flow in Arterial Structures. Part 2: Development of Coupled Fluid-Solid Algorithms*, Proc. Instn Mech. Engrs, **212** Part H (241-252), 1998.

[17] D. Tang, J. Yang, C. Yang, D. N. Ku, *A Nonlinear Axisymmetric Model with Fluid-Wall Interactions for Steady Viscous Flow in Stenotic Elastic Tube*, J. Biomech. Eng., **121** (494-501), 1999.

[18] M. Bathe, R. D. Kamm, *A Fluid-Structure Interaction Finite Element Analysis of Pulsatile Blood Flow Through a Complliant Stenotic Artery*, J. Biomech. Eng., **121** (361-369), 1999.

[19] L. Formaggia, J.-F. Gerbeau, F. Nobile, A. Quarteroni *On the Coupling of 3D and 1D Navier-Stokes Equations for the Flow Problems in Compliant Vessels*, INRIA, Rapport de Recherche nro 3862, 2000.

[20] P. G. Ciarlet, *Mathematical Elasticity,Volume I: Three-Dimensional Elasticity*, North-Holland, 1988.

[21] C. W. Hirt, A. A. Amsden, J.-L. Cook, *An Arbitrary Lagragian-Eulerian Computing Method for All Flow Speed*, J. Comp. Phys., **14** (227-253), 1974.

[22] L. P. Franca, S. L. Frey, T. J. R. Hughes, *Stabilized Finite Element Methods: I. Application to the Advection-Diffusive Model*, Comp. Meth. Appl. Mech. Eng., **95** (253-276), 1992.

[23] R. M. Lang, B. P. Cholley, C. Korcarz, R. H. Marcus, S. G. Shroff, *Peripheral Arterial and Aortic Diseases: Measurement of the Regional Elastic Properties of the Human Aorta: A New Application of Transesophageal Echocardiography with Automated Border Detection and Calibrated Subclavian Pulse Tracings*, Circulation, **90** (1875-1882), 1994.

[24] L. Formaggia, F. Nobile, A. Quarteroni, A. Veneziani, *Multiscale Modelling of the Circulatory System: A Preliminary Analysis*, Comp. and Vis. in Sci., **2** (75-83), 1999.

[25] F. Nobile, *Problemi di Interazione Fluido-Struttura in Emodinamica*, Thesis, Politecnico di Milano, 1997.

[26] K. Riemslagh, J. Vierendeels, E. Dick, *An Efficient Coupling Procedure for Flexible Wall Fluid-Structure Interaction*, Eccomas Congress on Comp. Meth. in Appl. Sci. and Eng., Barcelona, 2000.

[27] F. J. H. Gijsen, E. Allanic, F. N. van de Vosse, J. D. Janssen, *The Influence of the non-Newtonian Properties of Blood on the Flow in Large Arteries: Unsteady Flow in a* 90^o *Curved Tube*, J. Biomech., **32** (705-713), 1999.